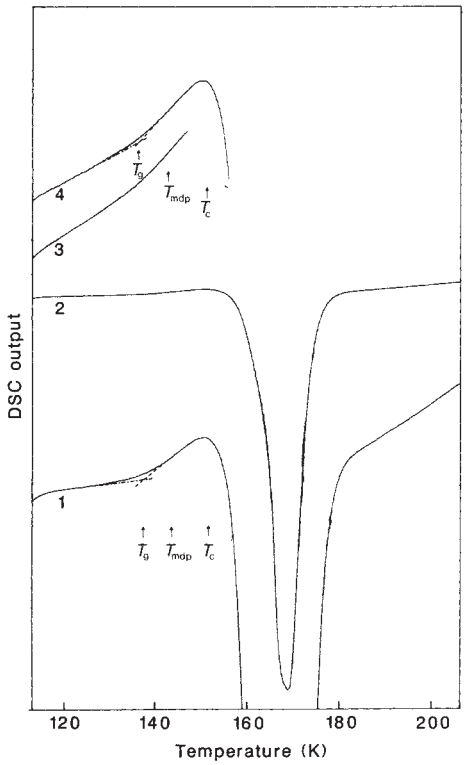

Fig. 2 The DSC scans of the hyperquenched glassy water prepared by using a 200 μm aperture. Curve 1 is for a 26.9 mg sample annealed at 130 K for 4 h, cooled to 103 K and heated. Curve 2 is the same as curve 1, but plotted on a reduced scale (1/8th). Curve 3 is for a 15.5 mg sample annealed at 130 K for 1.5 h and heated to 148 K. Curve 4 is for the same sample which was cooled immediately after curve 3 from 148 K to 103 K at a rate of 200 K min^{-1} while inside the calorimeter, then heated to 130 K, annealed for 1 h at 130 K, again cooled to 103 K, and finally heated for the DSC scan. The notations are the same as in Fig. 1. The heating rate was 30 K min^{-1}. The temperature axis is not corrected for the thermal lag of the instrument.

Se (ref. 15) or propanediol. Furthermore, the height of the glass-transition endotherm is much less than that observed for substances other than network type glasses[13].

The main difficulties in observing a glass–liquid transition in finely powdered materials containing trapped and/or absorbed gases is that during heating, (1) their surface energy decreases as a result of sintering and (2) gas molecules are desorbed from their surface. Vapour-deposited and pressure-amorphized materials often show this type of behaviour. For glasses in general, a further difficulty is caused by the spontaneous enthalpy relaxation, which for a hyperquenched glass appears as an exotherm (Fig. 1) at $T \ll T_g$ and continues up to T_g. For water in particular, rapid crystallization to cubic ice creates an additional difficulty by masking the relatively slow and small increase in the heat capacity that occurs at its T_g. These effects masked the glass-transition endotherm in a previous study[12]. Our procedure has removed these difficulties and revealed the glass transition in water and its thermodynamic reversibility.

These results are significant for understanding several aspects of amorphous ice and water, namely (1) the structural transition of the supercooled emulsified water, indicated by an approach towards a λ-type anomaly near 230 K (ref. 16), which makes it difficult to reconcile the structure of non-crystalline solid with that of liquid water[8], (2) the thermodynamic continuity of the structural states between water and its non-crystalline solids, if the postulated λ-type anomaly was absent[8] and (3) the polymorphism of amorphous solid water within the restrictions of hydrogen-bonded networks[8,17,18]. To help resolve some of these issues, we are currently studying the heat capacity of hyperquenched water and its transformation to other non-crystalline structures on compression at 77 K.

Financial support by the Forschungsförderungsfonds of Austria is gratefully acknowledged.

Received 22 June; accepted 2 October 1987.

1. Burton, E. F. & Oliver, W. F. *Proc. R. Soc.* **A153**, 166 (1935).
2. Sceats, M. G. & Rice, S. A. in *Water—A Comprehensive Treatise* (ed. Franks, F.) Ch. 2 (Plenum, New York, 1982).
3. Mishima, O. Calvert, L. D. & Whalley, E. *Nature* **310**, 393-395 (1984); **314**, 76-78 (1985).
4. Johari, G. P. & Jones, S. J. *Phil. Mag.* **54B**, 311-315 (1986).
5. MacFarlane, D. R. & Angell, C. A. *J. phys. Chem.* **88**, 759-762 (1984).
6. Handa, Y. P., Mishima, O. & Whalley, E. *J. chem. Phys.* **84**, 2766-2770 (1986).
7. Mayer, E. & Pletzer, R. *J. chem. Phys.* **80**, 2939-2952 (1984).
8. Johari, G. P. *Phil. Mag.* **35**, 1077-1090 (1977).
9. Angell, C. A. in *Water—A Comprehensive Treatise* (ed. Franks, F.) Ch. 1 (Plenum, New York, 1982).
10. Mayer, E. *J. appl. Phys.* **58**, 663-667 (1985); *J. phys. Chem.* **89**, 3474-3477 (1985).
11. Mayer, E. *J. phys. Chem.* **90**, 4455-4461 (1986).
12. Hallbrucker, A. & Mayer, E. *J. phys. Chem.* **91**, 503-505 (1987).
13. Wong, J. & Angell, C. A. in *Glass: Structure by Spectroscopy* Ch. 1 (Dekker, New York, 1976).
14. Johari, G. P. & Goldstein, M. *J. chem. Phys.* **53**, 4245-4252 (1971).
15. Stephens, R. B. *J. Non-Cryst. Solids* **20**, 75-81 (1976).
16. Angell, C. A., Shuppert, J. & Tucker, J. C. *J. phys. Chem.* **77**, 3092-3097 (1973).
17. Maddox, J. *Nature* **326**, 823 (1987).
18. Speedy, R. J. *J. phys. Chem.* **86**, 982-991 (1982).

Sonoluminescence from non-aqueous liquids

Kenneth S. Suslick & Edward B. Flint

School of Chemical Sciences, University of Illinois at Urbana-Champaign, 505 S. Mathews Avenue, Urbana, Illinois 61801, USA

Our understanding of the chemical effects of high-intensity ultrasonic irradiation of liquids is still quite limited. It is generally accepted that sonochemistry results from acoustic cavitation: the creation, growth, and implosive collapse of bubbles in ultrasonically irradiated liquids[1]. The mechanism of sonoluminescence in aqueous systems has been a matter of some dispute; recent discussions have suggested at least three possible origins: black-body emission[2], chemiluminescence from radical recombination[3], and electric discharge[4]. Few studies of non-aqueous sonoluminescence, however, have been conducted[5–7]. We present here the first spectrally resolved sonoluminescence spectra from hydrocarbon and halocarbon liquids. These spectra originate unambiguously from excited-state molecules created during acoustic cavitation. These high-energy species probably result from the recombination of radical and atomic species generated during the high temperatures and pressures of cavitation.

The sonoluminescence spectrum of dodecane originates from excited state C_2, specifically from the $d^3\Pi_g \rightarrow a^3\Pi_u$ transition—the so-called Swan band (Fig. 1). The four bands at 435, 465, 510 and 550 nm correspond to $\Delta v = +2, +1, 0$, and -1 of the vibrational manifold, respectively. The sonoluminescence spectra of mesitylene, 4-heptanone and *n*-butylcyanide are qualitatively similar to that of dodecane, but with lower intensities and slight changes in the relative intensities of the vibrational bands.

Swan band chemiluminescence is seen from hydrocarbons in a wide variety of conditions, including flames[8], shock tubes[9,10] shock pyrolysis[11], plasmas[12], laser ablation[13], and low pressure discharges[14]. Grebe and Homann[14] in their study of the gas-phase reactions of acetylene with oxygen and hydrogen atoms (C_2H_2/O/H) in a low-pressure discharge flow reactor, provided compelling evidence that one reaction responsible for the generation of $C_2(d^3\Pi_g)$ was

$$C + CH_2 \rightarrow C_2^* + H_2 \qquad (1)$$

For several reasons, this is also a plausible step in the sonochemical formation of $C_2(d^3\Pi_g)$. First, the pressures and

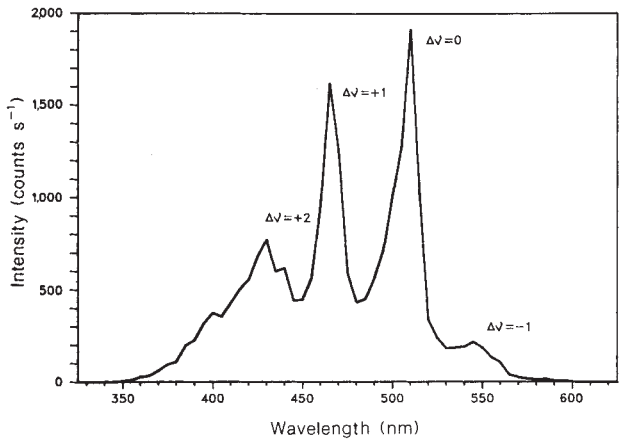

Fig. 1 The sonoluminescence spectrum of dodecane under argon. Emission is from excited state C_2 ($d^3\Pi_g \rightarrow a^3\Pi_u$). The cell temperature was −4°C; vapour pressure at this temperature[25] is 0.006 torr.

Methods. All chemicals and gases were purified by standard methods[26]. The irradiation cell has been described in detail elsewhere[27]; the source of ultrasound was a direct immersion titanium horn operating at 20 kHz, which produced a 1 cm diameter collimated beam (far field region) with intensity of ≈25 W cm^{-2} at the horn surface. Solutions were sparged with Ar during irradiation. Emitted light was collimated, passed into 0.25 m monochromator with 2.0 cm slits, and detected with a RCA 1P28 photomultiplier tube connected to a boxcar integrator. Spectra were collected at 5 nm increments and were not corrected for detector response.

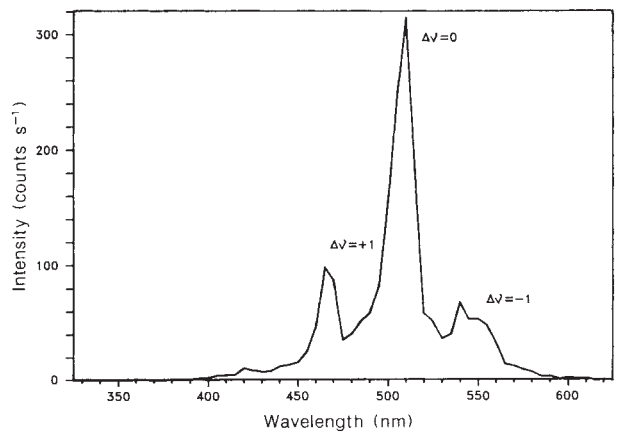

Fig. 2 The sonoluminescence spectrum of tetrachloroethylene under argon. Emission is from excited state C_2 ($d^2\Pi_g \rightarrow a^2\Pi_u$). The cell temperature was −16 °C; vapour pressure at this temperature[25] is 1.3 torr.

temperatures achieved during acoustic cavitation are similar to those reached in shock tubes and plasmas. The effective temperature reached during cavitation in alkane solvents was recently determined[15] to be ≈5,200 K in the gas phase and ≈1,900 K in the liquid region surrounding the collapsed bubble, when the total vapour pressure is 5 torr. Since the efficacy of cavitational collapse is inversely dependent on the total vapour pressure[16] the effective temperatures generated in these sonoluminescent systems (whose vapour pressures are much less than 5 torr) must be even higher. Second, carbon–carbon bond cleavage of alkanes and the formation of radicals from non-aqueous liquids during ultrasonic irradiation has been documented[16]. The sonolysis of even *n*-alkanes generates a wide variety of homolytic products via a radical chain pathway. Atomic carbon and CH_2 can be created through such mechanisms. Indeed, the final products observed[16] from alkane sonolysis include large amounts of H_2, CH_4 and C_2H_2, consistent with the observed sonoluminescence. Third, other techniques which generate comparable temperatures and pressures on a macroscopic scale also produce Swan band emission. For example, the shock tube pyrolyses of benzene[9] and acetylene[16] produced chemiluminescence spectra that could be assigned to $C_2(d^3\Pi_g)$, and when liquid benzene was shock compressed to between 24 to 63 GPa, emission from the Swan bands of C_2 was also observed[11].

The sonoluminescence spectrum of tetrachloroethylene is shown in Fig. 2. This can also be assigned to the C_2 ($d^3\Pi_g \rightarrow a^2\Pi_u$) Swan transition. The change in the relative vibrational band intensities and the strong diminution of the $\Delta v = +2$ band indicates a lower internal energy in C_2* for tetrachloroethylene than for dodecane. This is consistent with the decrease in cavitational heating observed with increased total vapour pressure[16]. Several systems involving organic halides produce C_2* chemiluminescence, including reactions with hydrogen atoms at low pressure[17], with sodium atoms in a heat-pipe-oven reactor[18], and with N_2O and sodium[19]. The formation of C_2* is attributed to the reaction shown in equation 2. The abstraction of a halogen atom by another atom (H or Na) generates the species that eventually luminesce. During ultrasonic irradiation, however, these radicals are formed by the high temperatures of the cavitation event. The sonochemistry of haloalkanes is little explored, although the sonolysis of chloroform to produce radicals and carbenes has been recently reported[20,21].

$$C + CCl \rightarrow C_2^* + Cl \qquad (2)$$

Figure 3 shows the sonoluminescence spectrum and the ultraviolet-visible absorption spectrum of nitroethane. The intense absorption of nitroethane at wavelengths below 375 nm prevents detection of any spectral features in the ultraviolet. This sonoluminescence emission can be assigned[22] to the NO emission bands from the $B^2\Pi \rightarrow X^2\Pi$ transition (the so-called β bands), with $\Delta v \geq 12$. The spectrum is *not* consistent with the chemiluminescence observed[23] from NO_2*, which is a broad emission from 400 to 1,200 nm with a maximum at about 650 nm. The reaction of carbon atoms with NO_2 (equation 3) has been studied in a low-pressure gas discharge reactor[24], and was identified as the only plausible mechanism for the formation of NO(β). This mechanism is consistent with those proposed for C_2* sonoluminescence.

$$C + NO_2 \rightarrow CO + NO(\beta) \qquad (3)$$

These sonoluminescence spectra of non-aqueous liquids demon-

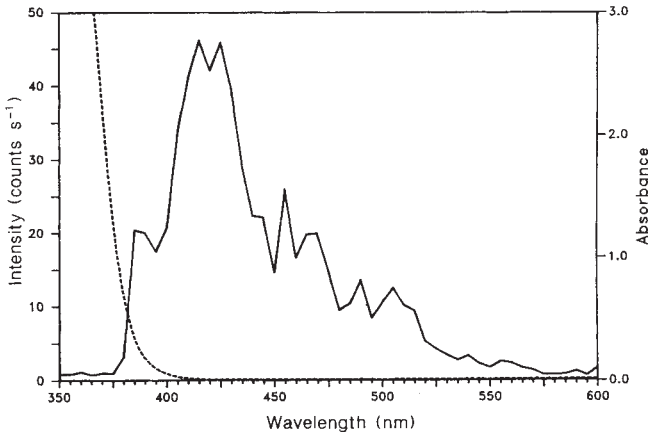

Fig. 3 The sonoluminescence spectrum of nitroethane under argon, scale at left. ———, Emission from excited state NO ($B^2\Pi \rightarrow X^2\Pi$). The cell temperature was −19 °C; vapour pressure at this temperature[25] is 1.1 torr. - - - - -, The ultraviolet-visible spectrum of nitroethane, 1 cm path length, absorption scale at right.

strate that ultrasound is a powerful chemical initiator and that significant chemistry occurs during ultrasonic irradiation even in the absence of reactive solutes. The similarity between sonoluminescence and the chemiluminescence seen with other high energy techniques (such as flames, plasmas, and shock tubes) indicates that similar chemistry is occurring during the ultrasonic irradiation of liquids.

We thank Dr A. Scheeline for assistance in instrument design, and the NSF for its support. K.S.S. gratefully acknowledges receipt of an NIH Research Career Development Award and of a Sloan Foundation Research Fellowship.

Received 5 June; accepted 24 September 1987.

1. Suslick, K. S. *Adv. organomet. Chem.* **25**, 73-119 (1986); *Modern Synthetic Methods* **4**, 1-60 (1986) (ed.) *Ultrasound: Its Chemical, Physical, and Biological Effects* (VCH, New York, 1987).
2. Walton, A. J. & Reynolds, G. T. *Adv. Phys.* **33**, 595-660 (1984).
3. Verrall, R. E. & Sehgal, C. *Ultrasonics* **25**, 29-30 (1987).
4. Margulis, M. A. *Ultrasonics* **23**, 157-169 (1985).
5. Chambers, L. *J. chem. Phys.* **5**, 290-292 (1937).
6. Jarman, P. *Proc. phys. Soc.* **73**, 628-640 (1959).
7. Golubnichii, P. I., Goncharov, V. D. & Protopopov, Kh. V. *Sov. Phys. Acoust.* **16**, 323-326 (1971).
8. Gaydon, A. G. *Spectroscopy of Flames* 2nd edn (Chapman and Hall, New York, 1974).
9. Kanoo, S. K. *Spectroscopy Lett.* **14**, 239-248 (1981).
10. Cooper, D. M. & Nicholls, R. W. *Proc. 10th Int. Shock Tube Symp.* (ed. Kamimoto, G.) 696-703 (Shock Tube Research Society, Tokyo, 1975).
11. Nicol, M., Johnson, M. L. & Holmes, N. C. *Physica* **139/140B**, 582-586 (1986).
12. Heinrich, G., Nickel, M., Mazurkiewicz, M. & Avni, R. *Spectrochimca Acta* **33B**, 635-647 (1978).
13. Anselment, M., Smith, R. S., Daykin, E. & Dimauro, L. F. *Chem. phys. Lett.* **134**, 444-449 (1987).
14. Grebe, J. & Homann, K. H. *Ber. Bunsenges. phys. Chem.* **86**, 587-597 (1982).
15. Suslick, K. S., Hammerton, D. A. & Cline, R. E. Jr *J. Am. chem. Soc.* **108**, 5641-5642 (1986).
16. Suslick, K. S., Gawienowski, J. W.; Schubert, P. F. & Wang, H. H. *J. phys. Chem.* **87**, 2299-2301 (1983): *Ultrasonics* **22**, 33-36 (1984).
17. Arnold, S. J., Kimbell, G. H. & Snelling, D. R. *Can. J. Chem.* **53**, 2419-2425 (1975).
18. Wang, X, Li, X. & Lou, N. *Chem. phys.* **61**, 25-33 (1981).
19. Luria, M., Eckstrom, D. J. & Benson, S. W. *J. chem. Phys.* **64**, 3103-3110 (1976).
20. Suslick, K. S. & Schubert, P. F. *J. Am. chem. Soc.* **105**, 6042-6044 (1983).
21. Henglein, A. & Fischer, C. H. *Ber. Bunsenges. Phys. Chem.* **88**, 1196-1199 (1984).
22. Young, R. A. & Sharpless, R. L. *J. chem. Phys.* **39**, 1071-1102 (1963).
23. Sutoh, M., Morioka, Y. & Nakamura, M. *J. chem. Phys.* **72**, 20-24 (1980).
24. Dorthe, G. *et al. J. chem. Phys.* **82**, 2313-2320 (1985).
25. Riddick, J. A. & Bunger, W. G. *Techniques of Chemistry* Vol. 2 (Wiley, New York, 1970).
26. Perrin, D. D., Armarego, W. L. F. & Perrin, D. R. *Purification of Laboratory Chemicals* 2nd edn (Pergamon, New York, 1980).
27. Suslick, K. S. & Flint, E. B. in *New Developments in the Synthesis, Manipulation and Characterization of Organometallic Compounds* (American Chemical Society, Washington, DC, in the press).

Stable Ga–Mg–Zn quasi-periodic crystals with pentagonal dodecahedral solidification morphology

Wataru Ohashi & Frans Spaepen

Division of Applied Sciences, Harvard University, Cambridge, Massachusetts 02138, USA

The discovery in 1984 by Shechtman and co-workers of an Al–Mn alloy phase that exhibited a sharply peaked diffraction pattern with icosahedral point symmetry ($m\bar{3}\bar{5}$) was a major development in crystallography[1]. It was the first demonstration that quasi-periodic structures with fivefold symmetry axes, which had been described in the mathematical literature and whose sharp reciprocal lattice peaks could be indexed with two sets of incommensurate basis vectors, did actually occur in nature. This discovery has been followed by intense experimental and theoretical work; many more icosahedral and decagonal crystals have been discovered, and the theory describing the quasi-periodic lattices and their defects was greatly developed[2–4]. With one exception, all quasi-periodic crystals that have been discovered until now are metastable; they are produced by non-equilibrium methods, such as melt quenching, ion-beam mixing and sputtering, and upon heating they transform to phases with a periodic crystal structure. The only stable quasi-periodic crystal that was known is found in the Al–Li–Cu system, and has a striking rhombic triacontahedral solidification morphology[5–7]. We report here the discovery in the Ga–Mg–Zn system of a second stable quasi-periodic crystal with a pentagonal dodecahedral solidification morphology.

Villars *et al.*[8] and Chen and Inoue[9] had reported that quasi-periodic crystals could be formed in the Ga-Mg-Zn system by rapid solidification. We prepared an icosahedral phase of composition $Ga_{1.0}Mg_{1.8}Zn_{2.1}$ by melt spinning. Figure 1 shows the characteristic electron diffraction pattern taken along the fivefold axis of one of the crystals. We discovered that this phase was stable by heating it in the differential scanning calorimeter. Figure 2 shows the result: no exothermal peaks, characteristic of the non-equilibrium transformation to a more stable phase, were observed; the endothermic peaks correspond to peritectic melting. The melting phenomena above 680K were confirmed by direct observation. Annealing of the icosahedral phase for 52 h at 638 K did not induce any transformations and left the electron diffraction pattern unchanged.

Based on this evidence for the thermodynamic stability of this icosahedral phase we concluded that it should be possible to obtain large crystals by slow cooling from the melt. We prepared several alloys that were solidified in a graphite mould under a helium–hydrogen atmosphere at a cooling rate of about 3K min^{-1}. Several crystals of the type shown in Fig. 3 were found in a shrinkage cavity at the top surface of an alloy with average composition $Ga_{1.0}Mg_{2.1}Zn_{3.0}$. The growth morphology of these crystals is pentagonal dodecahedral (not pyritohedral as is some-

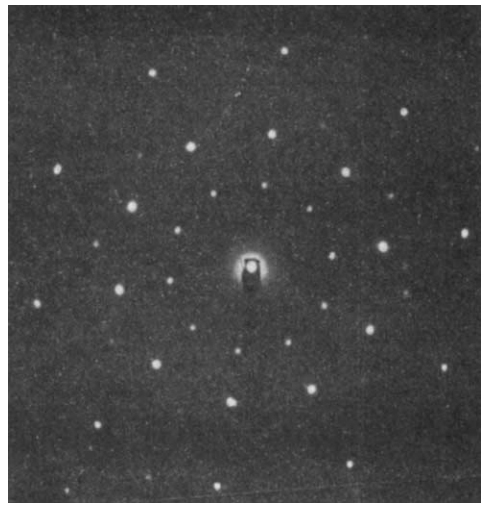

Fig. 1 Electron diffraction pattern from a $Ga_{1.0}Mg_{1.8}Zn_{2.1}$ icosahedral crystal in a melt-spun ribbon.

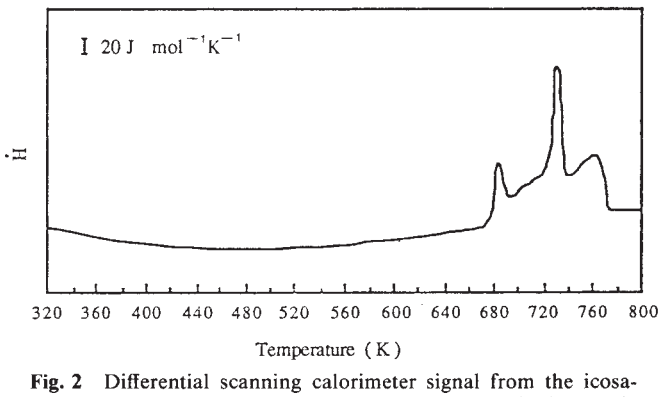

Fig. 2 Differential scanning calorimeter signal from the icosahedral $Ga_{1.0}Mg_{1.8}Zn_{2.1}$ phase produced by melt spinning. Only melting reactions are observed.